^{53}Cr($n,n'\gamma$) reactions and the level structure of ^{53}Cr

D. C. Larson and J. K. Dickens

Oak Ridge National Laboratory, Oak Ridge, Tennessee 37831

(Received 6 July 1988)

Gamma-ray decay of levels in the stable isotope ^{53}Cr has been studied using ^{53}Cr($n,n'\gamma$) reactions for incident neutron energies between threshold and 10 MeV. Measured gamma-ray production cross sections have been compared with earlier measurements and with cross sections calculated using precompound-compound-nucleus theory. Some of the present results are at variance with earlier experimental or evaluated results. For example, for the decay of the $E_x = 1537$-keV level we are unable to explain variations in the measured branching ratios of the transition gamma rays as a function of incident neutron energy. The experimental data were analyzed within the framework of several theoretical model calculations of the level structure of ^{53}Cr. Quantitative discrepancies are discussed.

I. INTRODUCTION

The level structure of the stable nucleus ^{53}Cr has been studied via inelastic nucleon scattering[1-9] as well as charged-particle reactions,[1-6,9-14] and gamma-ray transitions among levels have been observed by in-beam spectroscopy methods[2,8,13-31] and following beta decay[32,33] of ^{53}V. Recently, experimental data available through 1983 were compiled and evaluated by Peker[34] as part of the Nuclear Data Project. One might expect, therefore, that the low-lying (excitation energy $E_x < 3$ MeV) level structure of ^{53}Cr could be considered well known. One might also expect that the ^{53}Cr level structure can be satisfactorily described within the theoretical framework of the nuclear shell model. Reported calculations[35-45] exhibit reasonable agreements with experiment, at least for level excitation energies E_x and for calculated spins and parities J^π.

We have embarked upon a program[46] to provide experimental cross sections for gamma rays produced by energetic neutrons ($0.5 < E_n < 20$ MeV) interacting with stable nuclei in the mass region $A \sim 60$ for the purpose of providing data for comparisons with, and leading to improvement of, computations of reaction cross sections using nuclear models.[47,48] These calculations require knowledge of the level structure as well as the transition branching ratios of the decay of excited states for many nuclei in this mass region. We have measured gamma-ray yields for neutron interactions with ^{53}Cr as a part of this program. Most of the presently observed gamma rays can be placed as transitions among known levels of ^{53}Cr, and a detailed discussion of these placements is given in a recent laboratory report.[49] In addition to new information about gamma-ray decay of levels in ^{53}Cr, we have observed data on yields of the transition gamma rays from decay of the presumed well-known low-lying level in ^{53}Cr at $E_x = 1537$ keV which are *not in agreement* with what should be expected on the basis of current knowledge[34] of ^{53}Cr. Discussion in the present paper will highlight the results from both nuclear spectroscopic and nuclear reaction viewpoints.

II. EXPERIMENTAL DETAILS

The experimental system has been discussed in some detail in earlier reports.[46,49] The salient features are shown schematically in Fig. 1. A large-volume Ge(Li) detector was placed at 0.40 m from the sample at a scattering angle θ_γ of 125 deg. This angle was chosen because $P_2(125 \text{ deg})=0$, and so one may use the relationship between the angle-integrated total gamma-ray production cross section and the measured differential cross section:

$$\sigma(E_\gamma) \simeq 4\pi \, d\sigma(\theta_\gamma = 125 \text{ deg})/d\omega . \tag{1}$$

This equation is exact[50] if J of the decaying excited state is $\leq \frac{3}{2}$, and is a good approximation[27] for states in ^{53}Cr having larger J.

The other aspect of this choice of θ_γ is the Doppler effect on an observed gamma-ray energy. The Doppler effect is manifest in two ways: (1) variation of observed E_γ, and (2) shift of the mean E_γ of the (broadened) response so that the observed E_γ is not necessarily the true energy of the emitted gamma ray. The latter effect is well known and often used as a basis for level lifetime determination. The measured energy E_γ^{obs} is related to the intrinsic energy E_γ by the relationship

$$E_\gamma^{\text{obs}} = E_\gamma[1 + F(t)\beta_{\text{c.m.}} \cos\theta_\gamma] , \tag{2}$$

where $\beta_{\text{c.m.}}$ is the scalar velocity of the center of mass in units of c, and $F(t)$ is a function of t, the mean lifetime of the decaying level. The values of $F(t)$ range between 1 for $t < 10^{-15}$ s to 0 for $t > 10^{-12}$ s. As far as peak broadening is concerned, one may readily deduce that this broadening is a function of the angular distribution of the recoiling ion. If isotropy in the center-of-mass system of the neutron-scattering angular distribution is assumed, the Doppler-broadened linewidth is given approximately by

$$R \approx E_\gamma \beta_{\text{ion}} F(t) , \tag{3}$$

where β_{ion} is the scalar velocity of the ion in the center-

of-mass system. This Doppler linewidth must be combined with the intrinsic resolution of the detection system to obtain the observed resolution, which, in turn, must be known in order to determine if a given peak observed in the raw data could be due to detection of more than one gamma-ray transition.

The sample used was Cr_2O_3 encapsulated in a cylindrical nylon container of 2.9 cm diameter by 6.7 cm height, having a mass of ~ 49 g and an isotopic enrichment of 95.4% in the ^{53}Cr isotope. The remaining concentrations were 0.3%, 4.1%, and 0.2% for ^{50}Cr, ^{52}Cr, and ^{54}Cr, respectively.

Altogether, 18 4096-channel gamma-ray spectra corresponding to 18 neutron time-of-flight bins for E_n between threshold and 10 MeV, were studied to provide information presented in this report. One of these spectra is exhibited in Figs. 2 and 3.

For most values of E_γ we used previously[34] determined values which we consider to be "known" to better than the accuracies associated with our gamma-ray energy calibrations; other values of E_γ reported herein were determined by utilizing a nearby difference

$$E_\gamma^{\text{unknown}} = E_\gamma^{\text{known}} + \Delta E_\gamma \ , \tag{4}$$

where ΔE_γ is based on the known energy dispersion of the experimental system. Uncertainties dE_γ, assigned to deduced E_γ, include uncertainties associated with ΔE_γ of Eq. (4) as well as those due to Doppler effects [Eq. (2)] if

the mean lifetime, t, of the decaying level is not known.

Assignments of observed gamma rays as specific transitions among levels of ^{53}Cr were based on (1) prior knowledge[34] or (2) agreement of the experimental E_γ with the expected transition energy E_t, coupled with the experimental incident-neutron threshold. A given observed threshold was, of course, approximate because of the incident-neutron energy bin size; in addition, thresholds for gamma rays due to decay of high-spin states tended to be indistinct because of small values of σ near threshold. We were also concerned about the possibility of an incorrect threshold because the decaying excited state had a "long" mean lifetime ($t > 1$ nsec). No such isomeric state has been reported[34] for ^{53}Cr, and we do not adduce any long-lived level from our data.

The reduced data consist of cross sections $\sigma(E_\gamma, E_n)$ obtained for gamma-ray production in ^{53}Cr of discrete-energy gamma rays having energies E_γ by incident neutrons having energies E_n. The E_n for this experiment are values representing energy bins described by the bounds, E_{low} and E_{high}, which were deduced from the flight-time data.

A combination of data reduction techniques involving computer methods and manual methods was used to extract yields of gamma rays from the spectral data. Gamma ray attenuation by the sample was computed[51] using attenuation coefficients in the literature[52] for oxygen and chromium (the thin-walled nylon container was assumed to be oxygen for this purpose); the largest such correction
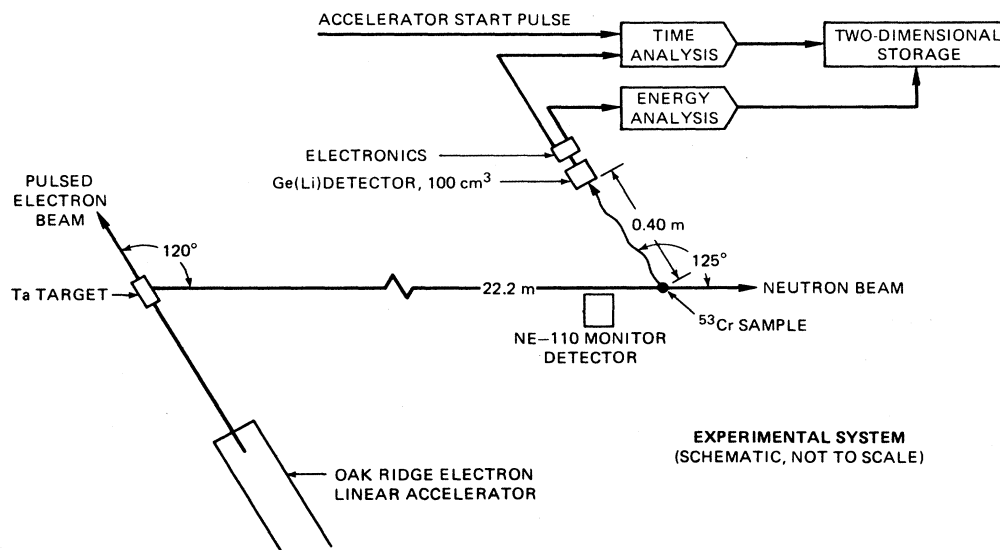

FIG. 1. Schematic representation of the experimental system. Starting from the lower left of this figure, 140-MeV electrons produced by the Oak Ridge Electron Linear Accelerator (ORELA) impinged upon a tantalum target producing bremsstrahlung. Neutrons produced in the Ta by subsequent photonuclear reactions were guided to the experimental area by an evacuated, 20-m-long flight tube located at 120 deg with respect to the incident electron beam. Collimators were inserted into the flight tube to define the neutron beam to a diameter of 7.3 cm at the sample position. The beam traveled ~ 2 m in air before impinging on the ^{53}Cr sample. A small NE-110 scintillator intercepted $\sim 1\%$ of the incident neutron flux and was used as a beam monitor. Two types of pulses were extracted from the detector electronics. One was for energy analysis using standard very-high-resolution pulse-amplitude analyzing equipment (3 μs time constants for the spectroscopy amplifier). The other pulse was used for fast-timing analysis to determine the flight time of the neutron responsible for the detected gamma ray. The time-of-flight datum was correlated with the energy datum in a data-acquisition computer, which sorted and then stored events on a bulk storage disk pack.
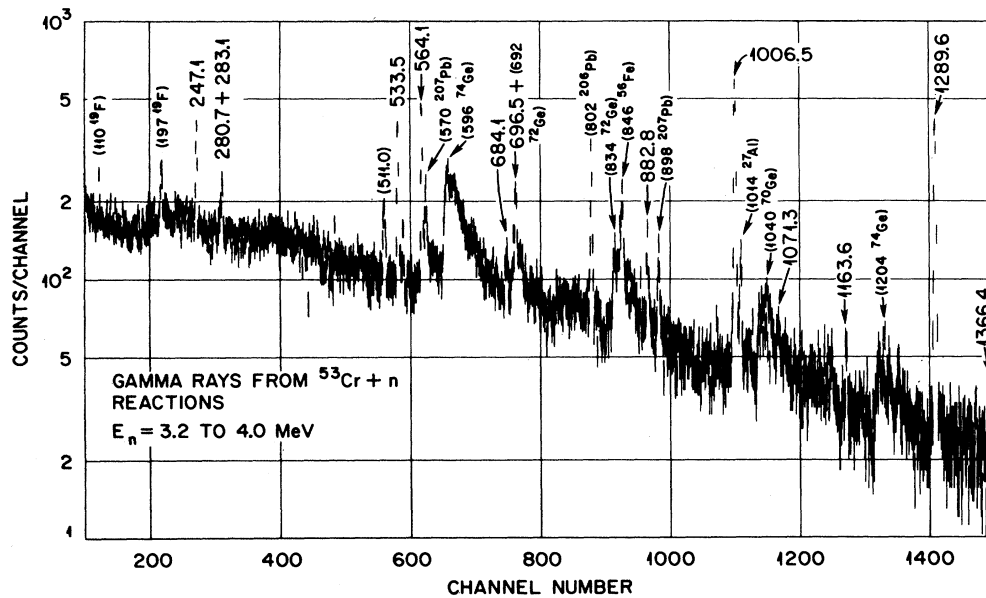
FIG. 2. Pulse-height spectrum for 3.2- to 4.0-MeV neutron interactions with the chromium sample. Gamma rays not due to $^{53}Cr(n,n')^{53}Cr$ are labeled with the isotope symbol. Neutron inelastic interactions with germanium isotopes result in broad peaks. The experimental dispersion is ~ 0.9 keV/channel.

was $\sim 17\%$ for $E_\gamma = 247$ keV. Multiple scattering effects were estimated by analytical methods and found to be $< 1\%$ for the present experiment. We were able to extract some $\sigma(E_\gamma, E_n)$ as small as 1 mb; however, for much of the data the lower limit to our sensitivity was ≥ 10 mb. The absolute normalization for σ is presently being checked in a similar series of measurements for a natural chromium sample.

III. ANALYSIS OF THE DATA

Prior experimental data support definite assignment of nine gamma-ray transitions among six levels in ^{53}Cr for $E_x < 2$ MeV; the adopted[34] levels, J^π, mean lifetimes, transitions, and branching ratios are shown in Fig. 4. Implied, but not explicit in this figure, are results from (γ, γ), $(p, p'\gamma)$, $(d, p\gamma)$, and (decay β, γ) coincidence
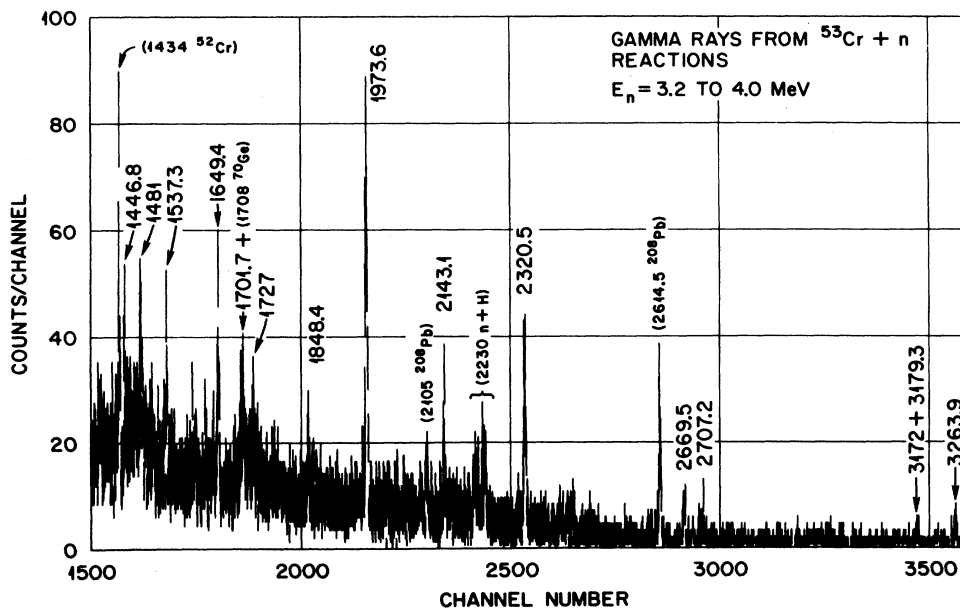

FIG. 3. Pulse-height spectrum of Fig. 2 continued to larger E_γ.

measurements (Refs. 2, 14, 16, 17, 22, 24, and 31–33) which have helped in defining the placements shown.

Gamma-ray production σ for $E_\gamma = 564$ keV deduced from the present experiment are exhibited and compared with previous measurements[15,25,27] in Fig. 5. Also shown in this figure are theoretical calculations using the statistical model code TNG (Ref. 53) combined with direct interaction contributions obtained using the DWUCK code.[54] Details of these calculations are given in a report by Shibata and Hetrick;[55] however, since the issuance of their report several additional calculations have been performed to cover specific aspects of the present study.

Probably the most important difference between the present experiment and the three earlier measurements[15,25,27] is that the latter measurements used natural chromium as samples (^{53}Cr isotopic abundance $\sim 9.5\%$). The present data agree reasonably well with the Bartol[15] and Lowell[27] data for E_n between 1.5 and 4 MeV, and are somewhat larger than the Bettis[25] data, not only for $E_\gamma = 564$ keV, but also for other gamma rays, as is discussed later on. We do not account for the substantial differences between present and earlier data for $E_n < 1.5$
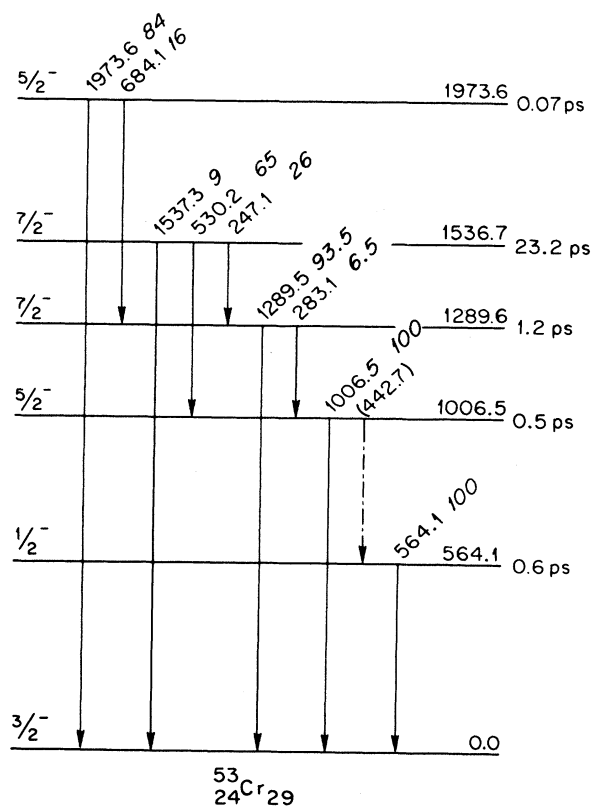
MeV.

Two theoretical curves are shown: the solid line represents direct (n,n') excitation of the $E_x = 564$ keV level; the dashed line represents the total excitation of this level including feeding by transitions from higher-lying levels in ^{53}Cr. For the present calculations, nuclear data (E_x, J^π, direct-interaction contributions, and gamma-ray transition branching ratios) were input for 14 states in ^{53}Cr up to $E_x = 2707$ keV; properties of "states" having larger E_x were treated[55] using level-density and spin-distribution computations.[53] For $E_n < 2.8$ MeV, indirect excitation of the 564-keV level is calculated explicitly from the specific level and branching-ratio information supplied to the code. For $E_n > 2.8$ MeV, the TNG code estimates indirect excitation based on empirically determined selection rules for postulated $E1$, $M1$, and $E2$ transitions from the deduced continuum of states.

As shown in Fig. 5, the present data are in better agreement with the calculated excitation function for $E_x = 564$ keV than are the earlier measurements,[15,27] and, in fact, suggest a resonance for $n + ^{53}$Cr at $E_n \sim 0.68$ (consistent with an observed resonance in the total cross section) and possibly another at ~ 1.0 MeV. For

FIG. 4. Level structure of ^{53}Cr for excitation energies, $E_x < 2$ MeV, taken from the compilation of Peker (Ref. 34). The 1006- to 564.1-keV transition, shown as the dot-dashed line, is not given in Peker's evaluation. The only experiment to report the $E_\gamma = 442.7$-keV gamma-ray decay of the $E_x = 1006$-keV level is a study (Ref. 32) of the decay of ^{52}V. We looked for evidence of this gamma ray in our data with negative results. Our data are interpreted as placing an upper limit of a 1% branching ratio for this transition.
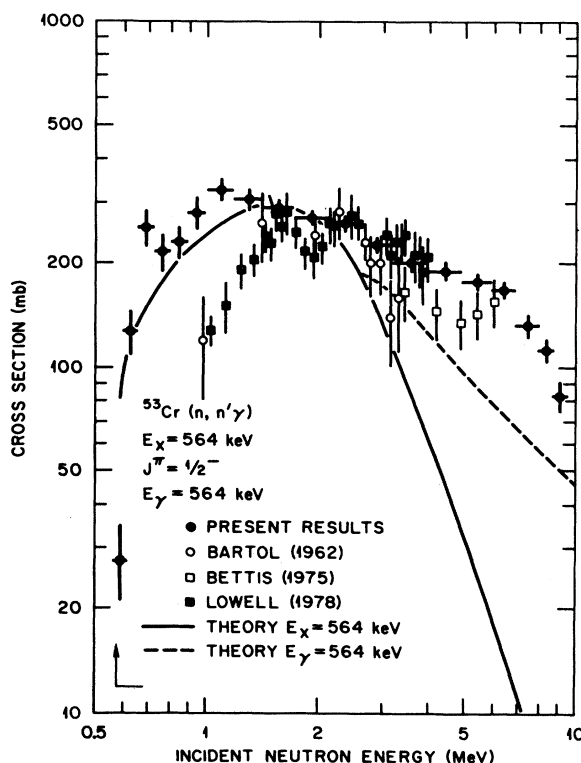

FIG. 5. Isotopic cross sections for production of the 564-keV gamma ray. The present data are compared with measurements performed at Bartol (Ref. 15), Bettis (Ref. 25), and Lowell (Ref. 27). The data are also compared with theoretical predictions (Ref. 55) for (a) direct inelastic excitation of the 564-keV level (solid line), and (b) total production of the 564-keV gamma ray (dashed line).

$E_n > 2.5$ MeV, all experiments suggest that there is more indirect excitation of the 564-keV level than estimated by the TNG program.

Gamma-ray production σ for $E_\gamma = 1006$ keV is shown in Fig. 6 and is compared with results of two earlier experiments[15,27] and with theoretical calculations. The Bettis results[25] for this gamma ray are much smaller and appear to be incorrect and so were not included in this figure. For $E_n > 1.5$ MeV, agreement with earlier measurements is quite good. In addition, the TNG program appears to provide a very good estimate of the indirect excitation from the postulated "continuum."

Cross sections for production of the 1290-keV gamma ray are shown in Fig. 7. Except for the Lowell data, agreement with earlier measurements is not quite as good as observed for $E_\gamma = 564$ and 1006 keV. The calculated indirect excitation follows the trend of the data, but somewhat underestimates this effect for E_n between 4 and 8 MeV. The onset of decreasing σ for $E_n \sim 8$ MeV observed in this figure and in Figs. 5 and 6 is likely related to the opening of the ^{53}Cr$(n,2n)$ channel which has a threshold at 8.1 MeV.

As indicated in Fig. 4, the 1290-keV level decay results also in a 283-keV gamma ray having a yield 7% of the yield for the 1006-keV gamma ray. This yield ratio should be a constant, independent of incident neutron energy, to within the approximations leading to Eq. (1). However, the first pass at these data yielded the results shown in Fig. 8. For most E_n, the yield ratio is very close to 7%. The variation near threshold involves relatively small peaks in the raw data and is believed to be due to experimental conditions. However, we have not been able to pin down the source and so the results are reported as obtained. More important are the results for E_n between 3 and 6 MeV. The raw data for the peaks corresponding to $E_\gamma \approx 283$ keV in several of the spectra are exhibited in the upper portion of the figure. The solid crosses in the lower portion of the figure were determined
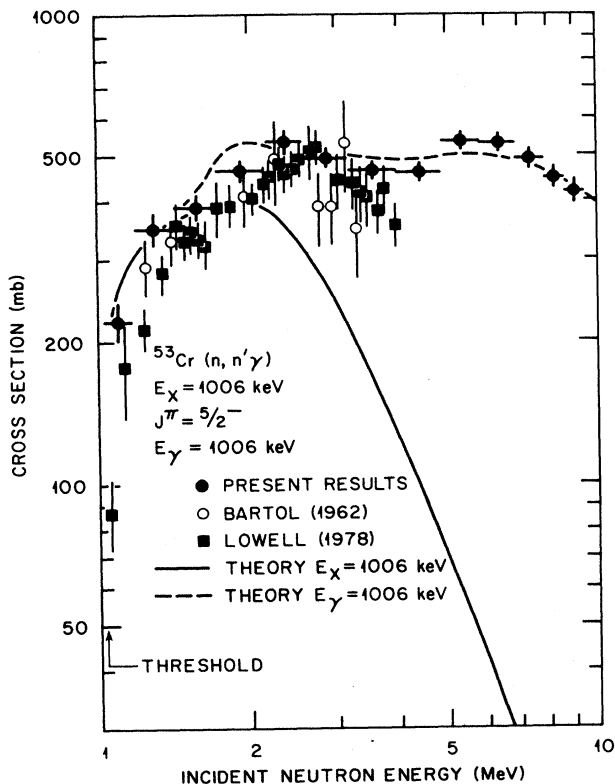

FIG. 6. Isotopic cross sections for production of the 1006-keV gamma ray. The present data are compared with measurements performed at Bartol (Ref. 15) and Lowell (Ref. 27). The data are also compared with theoretical predictions (Ref. 55) for (a) direct inelastic excitation of the 1006-keV level (solid line), and (b) total production of the 1006-keV gamma ray (dashed line).
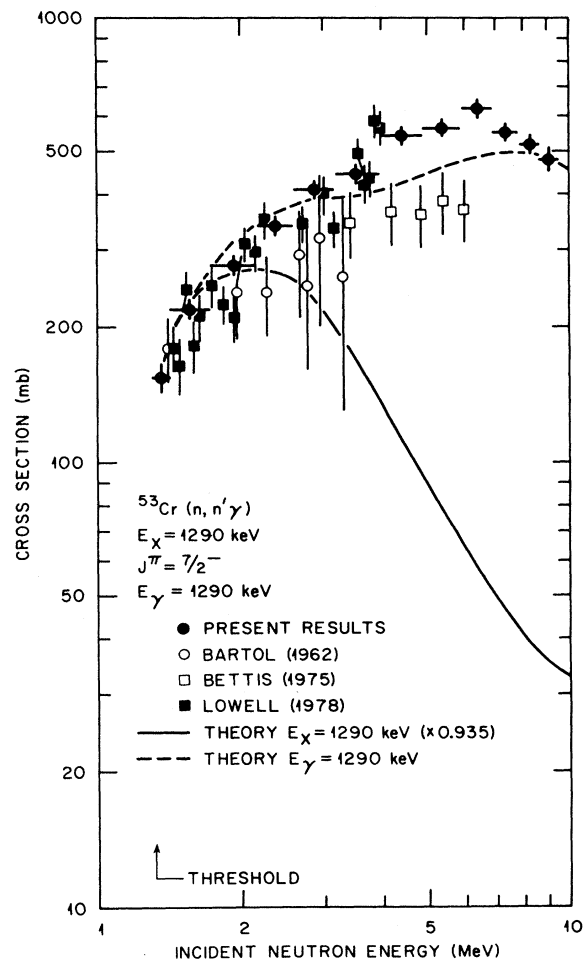
FIG. 7. Isotopic cross sections for production of the 1290-keV gamma ray. The present data are compared with measurements performed at Bartol (Ref. 15), Bettis (Ref. 25), and Lowell (Ref. 27). The data are also compared with theoretical predictions (Ref. 55) for (a) direct inelastic excitation of the 1290-keV level (solid line) multiplied by the branching ratio for the decay gamma ray, and (b) total production of the 1290-keV gamma ray (dashed line).

from integrating the full peak; however, as shown in the middle spectrum, the "peak" appears to be a doublet. Splitting this peak into two contributions results in the dashed cross for the yield for $E_\gamma = 283$ keV. Thus, it appears that the data support identification of a new transition gamma ray of ~ 281 keV. As discussed later, we suggest that this gamma ray is due to a transition of approximately this energy following decay of the 2453-keV excited state.

Our results for the decay of the next more energetic excited state in ^{53}Cr at $E_x = 1537$ keV are the most puzzling data in the present experiment. In the first place, as shown in Fig. 9, although our data for the dominant 530-keV transition agree well with the Lowell data,[27] the data do not agree well with the theory for the first 0.6 MeV above threshold. Indeed, the comparatively slow increase in the experimental excitation function is unlike any of the others observed in the present experiment. Evidently this state is "different" from that expected within the basic framework of the statistical model used in the calculations. More puzzling, however, are the extracted ratios of $\sigma(247$ keV$)/\sigma(530$ keV$)$ and

$\sigma(1537$ keV $)/\sigma(530$ keV$)$ which are shown as functions of incident neutron energy in Fig. 10. (For comparisons, these ratios from the data given in Fig. 4 are indicated by the light horizontal lines.) Because the results in Fig. 10 came from computer-extracted cross sections, the spectral data were carefully inspected. For $E_\gamma = 1537$ keV and for the energy bin $7.9 \leq E_n \leq 9.5$ MeV, the spectral data do not indicate any peak at all, hence the zero ratio shown in Fig. 10. Although there is no obvious peak in this spectrum, possibly a small peak might be deduced from a somewhat subjective appraisal of the raw data. Thus, the experimental ratios of the $E_\gamma = 1537$ keV to the $E_\gamma = 530$ keV transitions may well be consistent with 0.14 to within normal statistical uncertainties.

Careful study of the spectral data for $E_\gamma = 247$ keV, on the other hand, does not change the results shown in Fig. 10. The observed variations are not random, in the statistical sense, and we cannot believe they are due to experimental error. As discussed below, there are other experimental discrepancies involving decay of this state; at present we do not explain our observed results within the framework of the known level structure of ^{53}Cr.
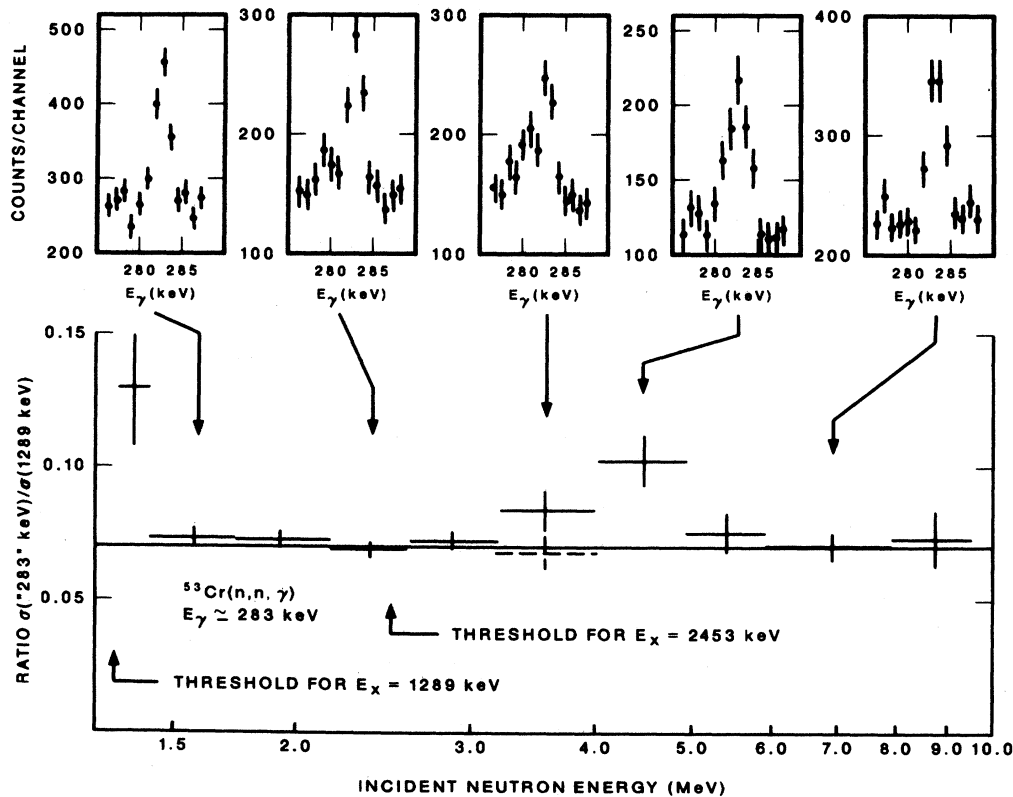

FIG. 8. Portions of spectral data for $E_\gamma \sim 283$ keV and ratios of the yields of the two transitions observed for decay of the $E_x = 1289.6$-keV level following ^{53}Cr$(n,n'\gamma)$ measurements as a function of incident neutron energy between threshold and 10 MeV. The upper portion of the figure exhibits portions of spectral data for five selected incident-neutron bins; the axis of abscissas for the separate spectra have been converted to gamma-ray energies for illustrative purposes. The lower portion of the figure exhibits the ratio data. The dashed cross for $3.2 \leq E_n \leq 4.0$ MeV indicates the value of the plotted ratio if only the main peak having $281 \leq E_\gamma \leq 285$ keV of the companion spectrum contributes to the yield for detection of a gamma ray having $E_\gamma = $ "283" keV. The horizontal line at ratio $= 0.07$ represents the adopted value from Peker's compilation (Ref. 34).

Data corresponding to the dominant ground-state decay of the 1974-keV level are shown in Fig. 11. The present results are shown for E_n only to 4 MeV because for larger E_n the peaks corresponding to $E_\gamma \sim 1974$ keV are definitely multiplets. Indeed, the peak corresponding to $E_\gamma \sim 1974$ keV for the neutron-energy bin 3.2–4.0 MeV appears to be a doublet; the plotted results shown in Fig. 11 exhibit two points for "present results;" the larger value represents the total peak yield, while the smaller value represents the peak yield for the larger contributor if the peak is actually a doublet. Interestingly, the Lowell data[27] also may indicate a second component, indirectly, having a threshold at ~ 3.5 MeV. Although the evidence is rather tenuous, there may be a second transition having $E_\gamma \approx 1970$ keV being observed. (A possible placement for such a gamma ray is as a transition between the $\frac{5}{2}^+$
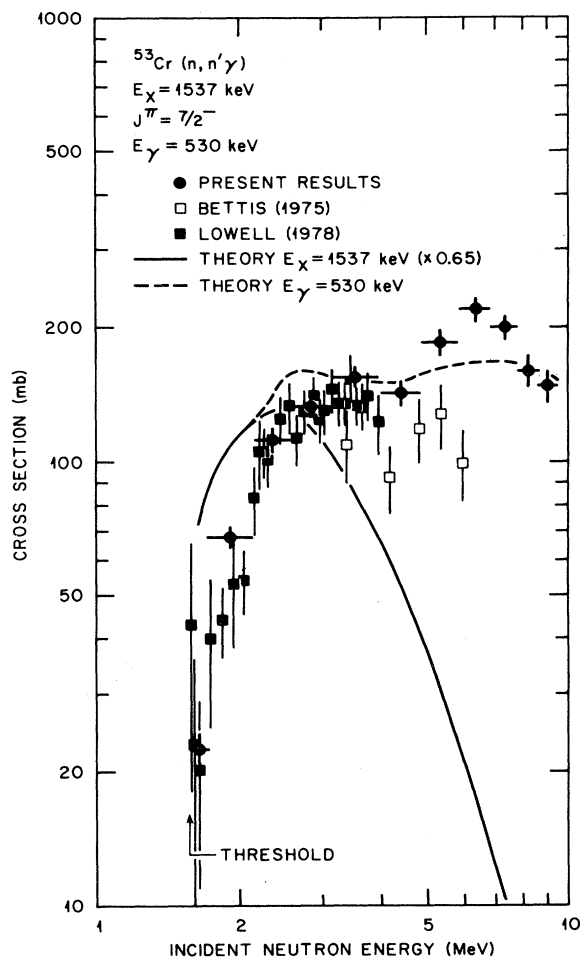

FIG. 9. Isotopic cross sections for production of the 530-keV gamma ray. The present data are compared with measurements performed at Bettis (Ref. 25) and Lowell (Ref. 27). The data are also compared with theoretical predictions (Ref. 55) for (a) direct inelastic excitation of the 1537-keV level (solid line) multiplied by the branching ratio for the decay gamma ray, and (b) total production of the 530-keV gamma ray (dashed line).

state at 3262 keV and the 1290-keV state.) Referring back to Fig. 11, there appears reasonable agreement among the experimental data and also with the theoretical results, at least to within assigned uncertainties.

The level structure for E_x between 2 and 3 MeV in ^{53}Cr is shown in Fig. 12. There are some differences between the level structure shown and that adopted in the Peker evaluation.[34] These include more precise energies for four levels and three additional transition gamma-ray placements. In addition, the "adopted" level at 2165 ± 10 keV is very likely the 2172-keV level and not a separate level, and the two "adopted" levels 2715 ± 10 and 2723 ± 10 keV, seen in two different experiments, are also very likely the same level.

Measurements of the cross sections for gamma-ray decay of the 2172-keV level are compared in Fig. 13 with calculated results. Agreement near threshold is excellent, and the substantially increasing calculated cross section for gamma-ray production is qualitatively correct; the data indicate increasing population of relatively high spin levels ($J \geq \frac{9}{2}$) which decay through the 2172-keV level. Similar results are observed for decay of the next more energetic level at 2233 keV, as shown in Fig. 14. One may note in passing that the 2172-keV level decays entirely to the $\frac{7}{2}^-$ level at 1290 keV; that is, not even a weak transition to the $\frac{7}{2}^-$ level at 1537 keV is observed. Conversely, the 2233-keV level decays only to the 1537-keV level.

Present results for the ground-state decay transition for $E_x = 2321$ keV are shown in Fig. 15, and for this level there is a definite discrepancy with prior experimental information. Patrawale and Kulkarni[26] report measuring, by Coulomb excitation, a $B(E2)$ value of 122 ± 14 e^2fm^4. This rather large value indicates a substantial[55] direct-interaction contribution to the excitation of this level by neutrons, and this contribution added to the statistical-model calculation is shown in Fig. 15 as the dot-dashed curve. The present data clearly disagree with the dot-dashed curve but are much closer to the statistical-model calculation shown by the solid curve, and, in fact, the data suggest very little indirect excitation of this level. We are unable to explain the discrepancy in, effectively, $B(E2)$ values between our results and the measurement of Patrawale and Kulkarni,[26] other than to note the latter measurement utilized a sample of natural chromium.

Finally, the 2453-keV level, which does not have an adopted J^π in Peker's evaluation,[34] will be discussed. According to Peker's evaluation,[34] this level decays by two transitions: $E_\gamma = 1446.8$ keV to the $J^\pi = \frac{5}{2}^-$ state at $E_x = 1006.5$ keV, and $E_\gamma = 1163.6$ keV to the $J^\pi = \frac{7}{2}^-$ state at $E_x = 1289.6$ keV, with relative branching ratios of 60:40. These branching ratios are based upon those reported by Carola et al.,[17] who give no details of their branching-ratio determination for this level in their report. As discussed above (see Fig. 8), our data indicate a new gamma ray having energy $E_\gamma \simeq 281$ keV with a threshold definitely < 3.2 MeV. The only transition energy, $\Delta E_x = E_x^{(1)} - E_x^{(2)}$, that is within ± 2 keV of this gamma-ray energy is the 2453-to-2172-keV transition. We have placed the $E_\gamma \simeq 281$-keV gamma ray as this
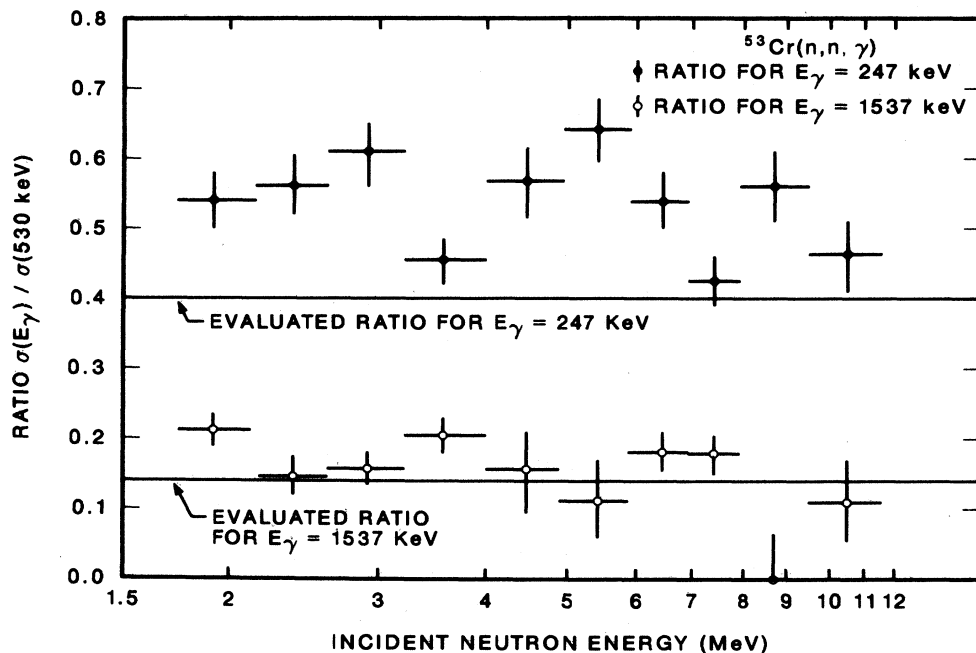
FIG. 10. Yield ratios for the three transitions observed for decay of the $E_x = 1536.7$-keV level following ^{53}Cr$(n,n'\gamma)$ measurements as a function of incident neutron energy between threshold and 11 MeV. The light horizontal lines represent the expected ratios (0.14 for $E_\gamma = 1537$ keV and 0.4 for $E_\gamma = 247$ keV) on the basis of adopted (Ref. 34) branching ratios as shown in Fig. 4.
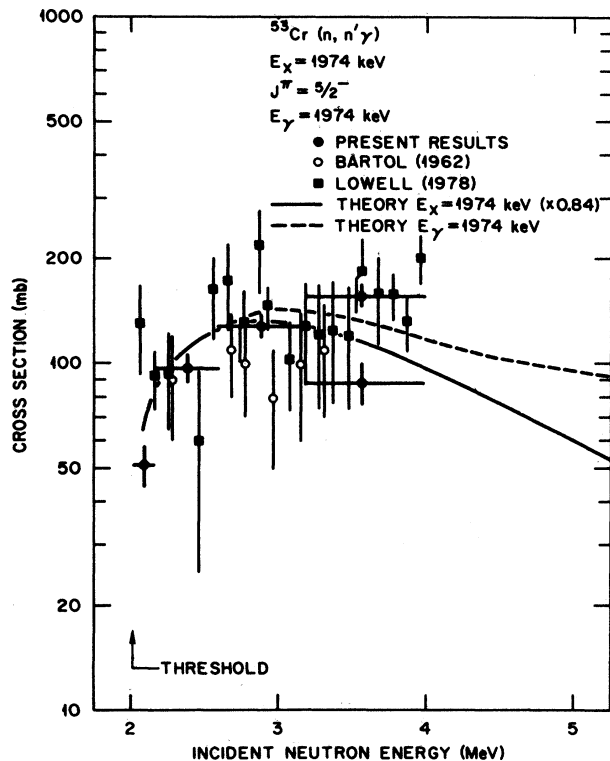

FIG. 11. Isotopic cross sections for production of the 1974-keV gamma ray. The present data are compared with measurements performed at Bartol (Ref. 15) and Lowell (Ref. 27). The data are also compared with theoretical predictions (Ref. 55) for (a) direct inelastic excitation of the 1974-keV level (solid line) multiplied by the branching ratio for the decay gamma ray, and (b) total production of the 1974-keV gamma ray (dashed line).

transition rather than postulating a new, heretofore unobserved level. If this placement is correct, then the spin of this state is very likely either $\frac{7}{2}$ or $\frac{9}{2}$, and the parity is almost surely negative.[49] On this basis, two statistical-model computations were performed, one for $J^\pi = \frac{7}{2}^-$ for $E_x = 2453$ keV and the other for $J^\pi = \frac{9}{2}^-$, and these are shown in Fig. 16 along with the data from the present experiment for the sum of the production cross sections for $E_\gamma = 1164$ and 1447 keV. Evidently, for E_n near threshold, the experimental results favor a $J^\pi = \frac{9}{2}^-$ assignment.

For higher-lying levels in ^{53}Cr, gamma-ray production cross sections are small and difficult to extract. We have placed 50 gamma rays (out of 65 observed) as transitions among 34 levels in ^{53}Cr up to an excitation energy of 4.36 MeV, including a new level at 3172 ± 3 keV decaying by a ground-state transition.[49] Some of these placements are indicated in Fig. 12.

In summary for this section, comparisons of cross sections have been made with earlier measurements[15,25,27] and with statistical-plus-direct-interaction-model predictions. The comparisons are generally favorable. The principal discrepancies observed are for excitation and decay of the 1537-keV level.

IV. DISCUSSION OF RESULTS

Analyses of the present data indicate that the statistical-model calculations using the TNG code do give a reasonable representation for most of the photon production excitation functions we measured. Indeed, in the absence of experimental measurements one may have to rely on calculations of this type, and the present comparisons lend confidence to calculational results, at least for

applied purposes. There are, however, some clearly disturbing discrepancies, particularly for $E_x = 1537$ keV, and to a lesser extent for $E_x = 2321$ keV. One may reasonably inquire whether current theoretical frameworks could provide a better understanding of these levels and assist in resolving these discrepancies.

As discussed in the Introduction, several structure calculations have been reported[35–45] for nuclei having 29 neutrons. The results of the 11 calculated level structures of ^{53}Cr are summarized in Fig. 17. This figure also includes the adopted levels of Peker's evaluation[34] in column (a).

Since the full shell-model treatment, using for example ^{40}Ca as the core, is intractable, more restrictive models have been used. These fall into three classes: (1) a shell

model assuming a ^{48}Ca core with the four valence protons restricted to the $f_{7/2}$ shell and the valence neutron allowed in the $p_{3/2}$, $f_{5/2}$, and $p_{1/2}$ shells, as done for results shown in columns (b),[35] (d),[37] (e),[38] (h),[41] (i),[42] and (l);[45] (2) a unified model in which the valence neutron is coupled to core states of ^{52}Cr, as done for results shown in columns (c),[36] (f),[39] (g),[40] and (h);[41] and (3) a shell model using ^{56}Ni as the core, with states constructed from four proton holes in the $f_{7/2}$ shell and either (a) the valence neutron in the $p_{3/2}$, $f_{5/2}$, or $p_{1/2}$ shells, or (b) a second neutron promoted from the $f_{7/2}$ shell to the valence shells, as done for results shown in columns (j) (Ref. 43) and (k) (Ref. 44).

These calculations taken together share some commonalities as well as exhibit diversities. The lowest-lying levels nearly all have the spin sequence $\frac{3}{2}$-$\frac{1}{2}$-$\frac{5}{2}$ in agreement with experiment, but the predicted level excitations are only in approximate agreement with experiment.
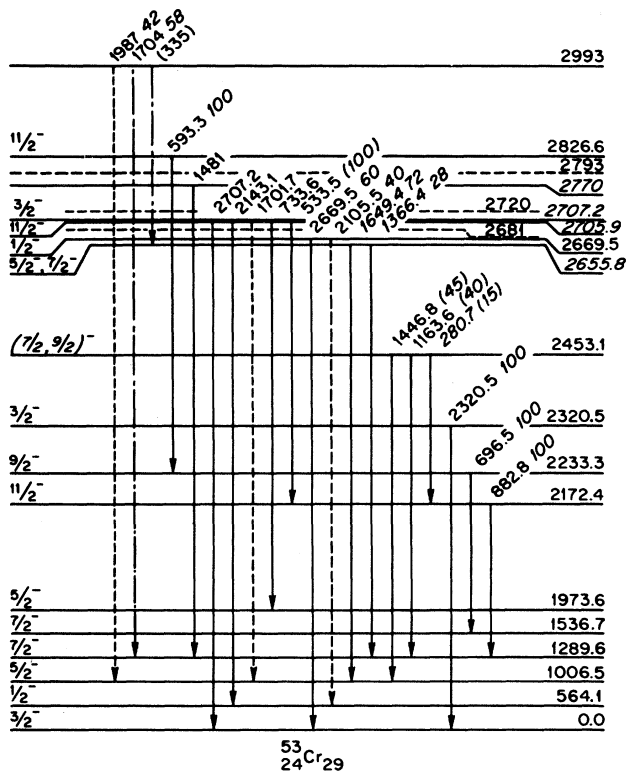

FIG. 12. Level structure of ^{53}Cr for excitation energies $E_x < 3$ MeV. This figure exhibits information obtained partly from Peker's compilation (Ref. 34) and partly from the present experiment. The four italicized level energies, three gamma-ray energies, and one J^π are new information from the present experiment. The dashed horizontal lines represent levels in the compilation for which decay transitions have not been observed. As mentioned in the text an adopted "level" at 2165 ± 10 keV is not included in this figure, and, in addition, two adopted "levels" at $E_x = 2715 \pm 10$ keV and 2723 ± 10 keV are shown here as a single level. The solid arrows indicate presently observed transitions, the three dashed arrows indicate transitions previously reported but not confirmed in the present experiment, and the two dot-dashed arrows indicate transition gamma rays which may have been detected in the present experiment but for which definitive assignments are uncertain.
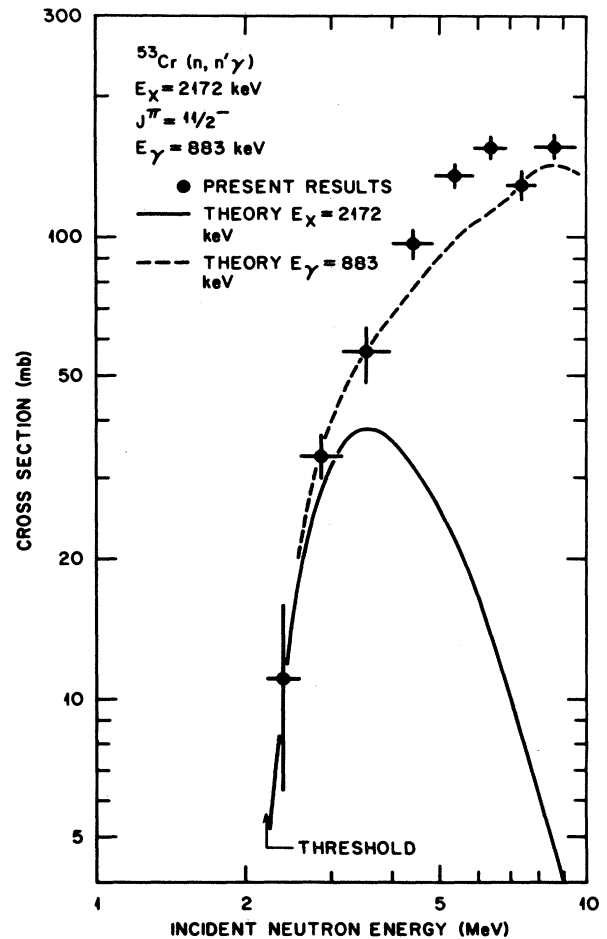

FIG. 13. Isotopic cross sections for production of the 883-keV gamma ray. The data are compared with theoretical predictions (Ref. 55) for (a) direct inelastic excitation of the 2172-keV level (solid line), and (b) total production of the 883-keV gamma ray (dashed line).

However, only two of these calculations, column (j) (Ref. 43) and (k) (Ref. 44), include a second low-lying $J^\pi = \frac{7}{2}^-$ state to match experiment, although Larner[40] [column (g)], predicts a second $J^\pi = \frac{5}{2}^-$ level close to $E_x \sim 1.5$ MeV. Another aspect easily observed in Fig. 17 is that *all* levels have negative parity, and indeed, experimentally the lowest-lying positive-parity level is the $J^\pi = \frac{5}{2}^+$ state at $E_x = 3262$ keV.[34]

These features are, of course, due to the choices of bases for the calculations. The ability of the first class of model to reproduce levels of the correct spin and parity near their experimentally observed counterparts depends to a large extent on determining the two-body matrix elements. In the cases where the matrix elements are obtained from fitting to observed levels in nearby nuclei the results are better than using calculated matrix elements based on some assumption about the two-body force. This difference in matrix elements is, in fact, the major difference among the shell-model calculations in this class. Maxwell and Parkinson,[37] column (d), calculated the required two-body matrix elements using a central force and not including spin-orbit or tensor effects. They obtained results of qualitative agreement with experiment. However, Vervier,[35] Ohnuma,[38] Carola and Ohnuma,[41] Horie and Ogawa,[42] and McGrory[45] obtained the matrix elements from fitting to levels with known spin and parity in nearby nuclei and obtained calculated results in better agreement with experiment. Matrix elements obtained via this method are assumed to contain effects of spin-orbit and tensor forces, as well as configuration mixing effects from orbits outside the calculational space. Except for missing the $\frac{7}{2}^-$ state at $E_x = 1.54$ MeV observed in (p,d), the low-lying level structure predicted by these calculations are in reasonable agreement with known levels observed by us and others. The identification of higher-lying experimentally observed levels with the calculated counterparts is not so clear.

Calculations using the unified model treat ^{53}Cr as a neutron (allowed in the $p_{3/2}$, $f_{5/2}$, and $p_{1/2}$ orbits) coupled to core states of ^{52}Cr. The main differences among
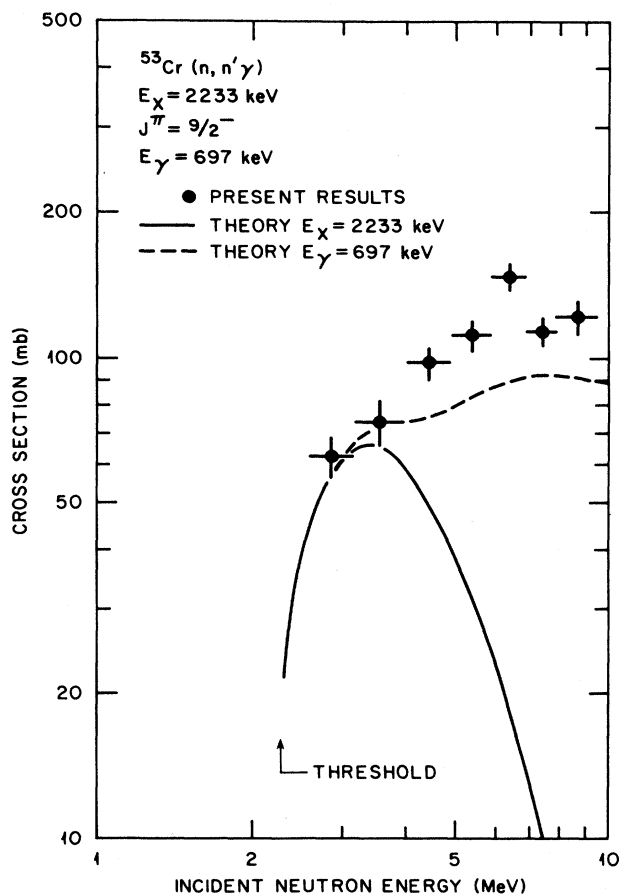

FIG. 14. Isotopic cross sections for production of the 697-keV gamma ray. The data are compared with theoretical predictions (Ref. 55) for (a) direct inelastic excitation of the 2233-keV level (solid line) and (b) total production of the 697-keV gamma ray (dashed line).
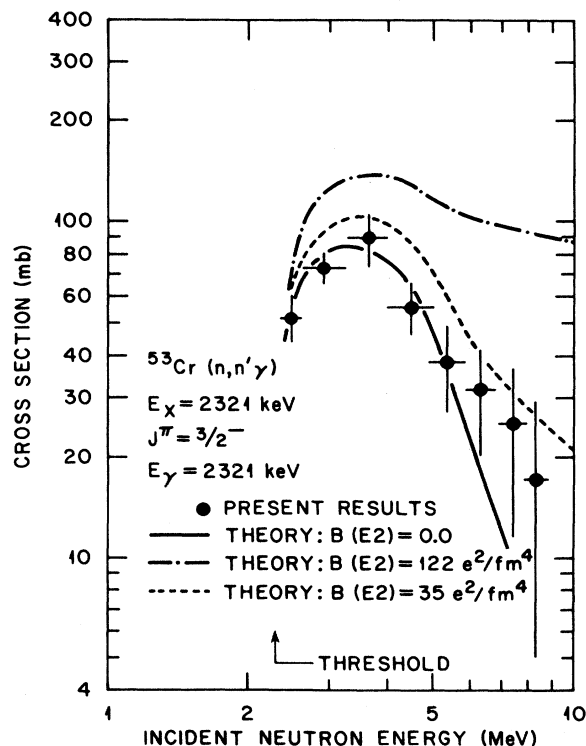

FIG. 15. Excitation function for the $E_\gamma = 2321$-keV gamma ray corresponding to the ground-state decay of a level at $E_x = 2321$ keV. The present isotopic cross sections are compared with theoretical predictions for (a) direct compound-nucleus excitation of the 2321-keV state (solid line), (b) direct-interaction excitation added to the compound-nucleus excitation (dot-dashed line) as deduced by Shibata and Hetrick (Ref. 55) based on the $B(E2)$ reported for this state by Patrawale and Kulkarni (Ref. 26), and (c) direct-interaction excitation based on a smaller value of $B(E2)$ predicted by Carola and Ohnuma (Ref. 41) added to the compound-nucleus excitation (dotted line).

these calculations are found in the descriptions of the coupling forces and the number of states of ^{52}Cr to which the neutron is coupled. Ramavataram,[36] column (c), and Carola and Ohnuma,[41] column (h), assumed that the ^{52}Cr core was a perfect vibrator, and coupled core states up to and including three phonons to the valence neutron. Rather than taking the phonon energy $\hbar\omega$ as the energy of the first excited state in ^{52}Cr, it was, along with the single-particle energies of the $p_{3/2}$ and the strength of the coupling interaction, treated as a free parameter. The calculations of Carola and Ohnuma,[41] column (h), provide energy levels and spectroscopic factors in rather good agreement with experimental information, at least up to 2.5 MeV. However, the electromagnetic properties are in only qualitative agreement with experiment. For example, their calculation places the second excited $J^\pi = \frac{3}{2}^-$ level at $E_x = 2.01$ MeV, identified with the experimental $J^\pi = \frac{3}{2}^-$ level at $E_x = 2.32$ MeV. For this state, the predictions include branching ratios of 25% each for transitions to the first $\frac{1}{2}^-$ and first $\frac{5}{2}^-$ states. Experimentally these transitions are not observed in our data. The calculation predicts for the model state a $B(E2) = 35$ e^2fm^4. Using this value for $B(E2)$ to determine the

direct-interaction contribution to the cross sections for the 2321-keV gamma-ray results in the dotted curve shown in Fig. 14. While the results for this value of $B(E2)$ agree reasonably well with the present data—certainly better than the excitation function computed for the larger $B(E2)$ of Patrawale and Kulkarni[26] does—the experimental evidence indicates no indirect excitation of the 2321-keV level. However, the model predicts indirect excitation of this level due to transitions from decay of higher-lying levels in the model scheme. Consequently, on the basis of the present measurements, one may question identifying this experimental level at $E_x = 2.32$ MeV with the model-predicted level at $E_x = 2.01$ MeV.

The unified model calculations of Philpott and True,[39] column (f), and Larner,[40] column (g), are more general in that the specific form of the core states is not specified, and the resulting matrix elements are treated as free parameters. Their purposes included a better understanding of the low-lying levels, so they couple the valence neutron only to the ground and first excited states of ^{52}Cr. The necessary parameters are adjusted to provide a calculated level structure having a good fit to experimentally known energy levels and spectroscopic factors from ^{53}Cr. Consequently, the energy levels are quite well reproduced, as are the electromagnetic properties; however, the spectroscopic factors are in only qualitative agreement with experiment. Since the model space is quite restricted, the number of experimentally observed levels is significantly underpredicted. As noted by these authors, this model is hard to extend, either by adding more complexity to the interaction or by including more core states in ^{52}Cr, since the number of matrix elements to be determined from the data would become too large.

The last class of structure calculations is also based on the shell model, using ^{56}Ni as the core. In each case, the protons are treated as four holes in the $f_{7/2}$ orbit, while the neutrons are treated in two ways. In the work of Benson and Johnstone,[43] column (j), the valence neutron is allowed to populate the $p_{3/2}$, $f_{5/2}$, and $p_{1/2}$ orbits, (giving a ^{53}Cr model similar to the other shell-model calculations), but in addition, the possibility of a neutron moving from the filled $f_{7/2}$ orbit to couple with the valence neutron is allowed. Thus, this model is the only one which can account for the state at 1.54 MeV as a $\frac{7}{2}^-$ hole state in ^{53}Cr, and the model further predicts other hole states having $J^\pi = \frac{9}{2}^-$, $\frac{11}{2}^-$, etc. We observe several of these levels (1.54 MeV, $\frac{7}{2}^-$; 2.23 MeV, $\frac{9}{2}^-$; and 2.83 MeV, $\frac{11}{2}^-$) and find that the $\frac{11}{2}^- \rightarrow \frac{9}{2}^-$ and $\frac{9}{2}^- \rightarrow \frac{7}{2}^-$ transitions are each pure transitions; no gamma rays to other states are observed. (The excitation function for the $\frac{9}{2}^- \rightarrow \frac{7}{2}^-$ transition is shown in Fig. 14.)

The work of Mooy and Glaudemans,[44] column (k), is based on the same basic model as the work of Benson and Johnstone,[43] but has no restriction on configuration mixing within the space used, thus allowing more configurations to contribute. They calculate excitation energies as well as electromagnetic transition rates and moments and obtain the best overall agreement of any of the calculations for excitation energies with experiment.
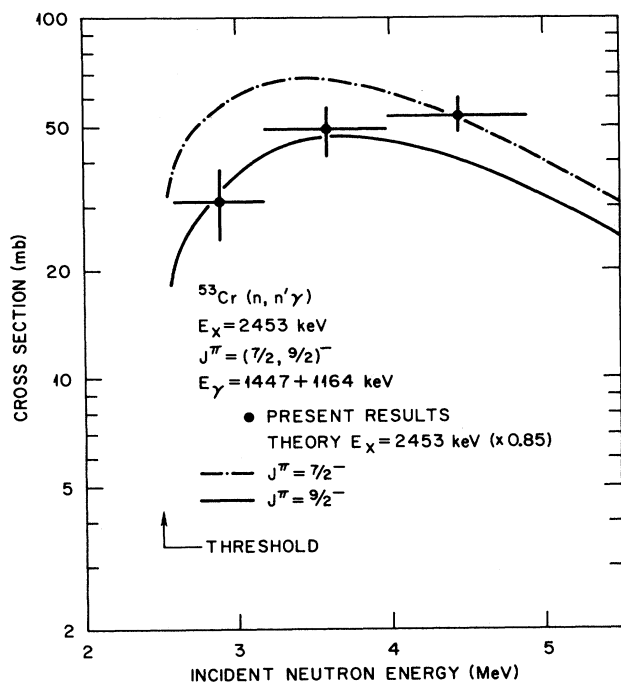

FIG. 16. Isotopic cross sections for the sum of the production of the 1164-keV and 1447-keV gamma rays. The data are compared with statistical-model predictions of cross sections for direct inelastic excitation of the 2453-keV level (a) on the basis that J^π for this level is $\frac{7}{2}^-$ (dot-dashed line), and (b) on the basis that $J^\pi = \frac{9}{2}^-$ (solid line). Both calculations have been multiplied by 0.85, the branching deduced from the present experiment (see Fig. 12). A theoretical calculation on the basis that $J^\pi = \frac{5}{2}^-$ is reported in Ref. 55, and it results in computed cross sections ~ 10% larger than those exhibited for $J^\pi = \frac{7}{2}^-$ in this figure.

They use criteria based on excitation energies and magnitudes of electromagnetic observables to identify selected levels as potential members of rotational bands corresponding to an axially symmetric rotor model. From these results they make several predictions on which we can comment based on our data.

From their rotational band analysis, they identify their second $\frac{7}{2}^-$, $\frac{9}{2}^-$, and $\frac{13}{2}^-$, and third $\frac{11}{2}^-$ levels as forming an excited $k = \frac{7}{2}$ band. The lowest member of the band is identified with the $\frac{7}{2}^-$ hole state at 1537 keV, and they note that this band contains states which in their model space are dominated by p-h excited configurations. We observe a gamma-ray cascade from the $(\frac{13}{2}^-)$ level at 3592 keV through the $\frac{11}{2}^-$ level at 2827 keV, the $\frac{9}{2}^-$ level at 2233 keV, and to the $\frac{7}{2}^-$ level at 1537 keV, as did Gullholmer and Sawa;[22] in addition, we obtain gamma-ray production cross sections for the $(\frac{13}{2}^-)$ and $\frac{9}{2}^-$ levels. However, the model also predicts a deformation parameter, β, used for the direct interaction component of the excitation of the 1537-keV level to be $\beta = 0.40$. The calculated excitation function shown in Fig. 9 used $\beta = 0.07$;

a calculation using $\beta = 0.40$ would overpredict the data even more than shown in this figure.

The results of Benson and Johnstone[43] and Mooy and Glaudemans[44] in which they calculate properties of the 1537-keV $\frac{7}{2}^-$ state are of particular interest in light of the difficulty in understanding this level experimentally. Besides the difficulties with our measurements noted in Figs. 9 and 10, consider the lifetime for this level, given as 23 psec in Peker's evaluation.[34] Two measurements are reported, both using the ^{50}Ti$(a,n\gamma)^{53}$Cr reaction; Engelstein et al.[23] obtained $t = 21.5 \pm 3.5$ psec while Radford and Poletti[29] obtained $t = 33.2 \pm 1.6$ psec for this level. However, as noted by Auble[57] a value for $t = 25$ psec is inconsistent (about a factor of 30 too large) with the experimental $B(E2) = 18 \pm 2$ e^2fm^4 for $E_\gamma = 1537$ keV deduced from Coulomb excitation measurements.[26] In addition, previously measured branching ratios[17,19,22,24,28,30] for the three decay modes exhibit large disagreements, at least in comparison with assigned uncertainties not only with the present data but also among themselves. With regard to the lack of agreement between the calculated
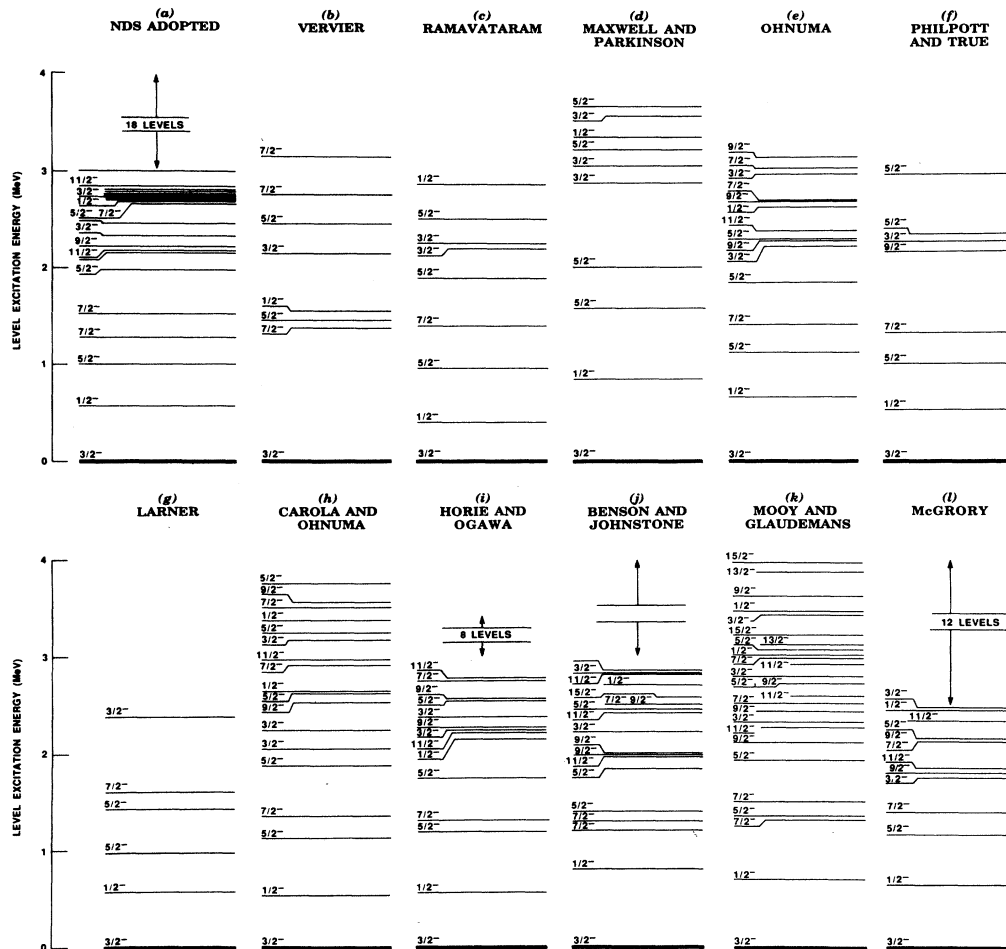

FIG. 17. Comparison of experimental level structure of ^{53}Cr according to Peker's evaluation, column (a) (Ref. 34), with calculated level structures from 11 studies, given in columns (b)–(l) (Refs. 35–45, respectively).

excitation function and the experimental data for this level as shown in Fig. 9, one may ask what physically determines the rate of rise in the computed excitation function for the crucial energy region from threshold to ~ 1 MeV above threshold. In the statistical model[58] the important variables are the transmission coefficients which are computed[59] using the optical model; the important quantum numbers are the J^π of the initial and final states of the inelastic scattering reaction. For the calculated excitation functions shown in Figs. 5–7, 9, 11, and 13–16, $J^\pi = \frac{3}{2}^-$ was used for the initial (ground) state of ^{53}Cr, and the evaluated[34] J^π were used for the excited states having E_x up to ~ 2.7 MeV. One aspect of this model is that the computed excitation functions for the two close-lying

$J^\pi = \frac{7}{2}^-$ states having $E_x \sim 1.5$ MeV will be very similar as a function of $E' = E_n - E_{\text{threshold}}$. The disagreement shown in Fig. 9 comes about because the *experimental* excitation functions for these two states are not very similar as a function of E'.

Could it be that $J^\pi \neq \frac{7}{2}^-$ for $E_x = 1537$ keV? To check on this possibility calculations were carried out for other possible, *however unlikely*, J^π assignments to this level, and the results are exhibited in Fig. 18. In particular, for $E_n < 3$ MeV it is apparent that none of the four excitation functions for negative-parity assignments agrees well with experiment. The best agreement was obtained for $J^\pi = \frac{7}{2}^+$ as shown by the dashed curve in this figure. We
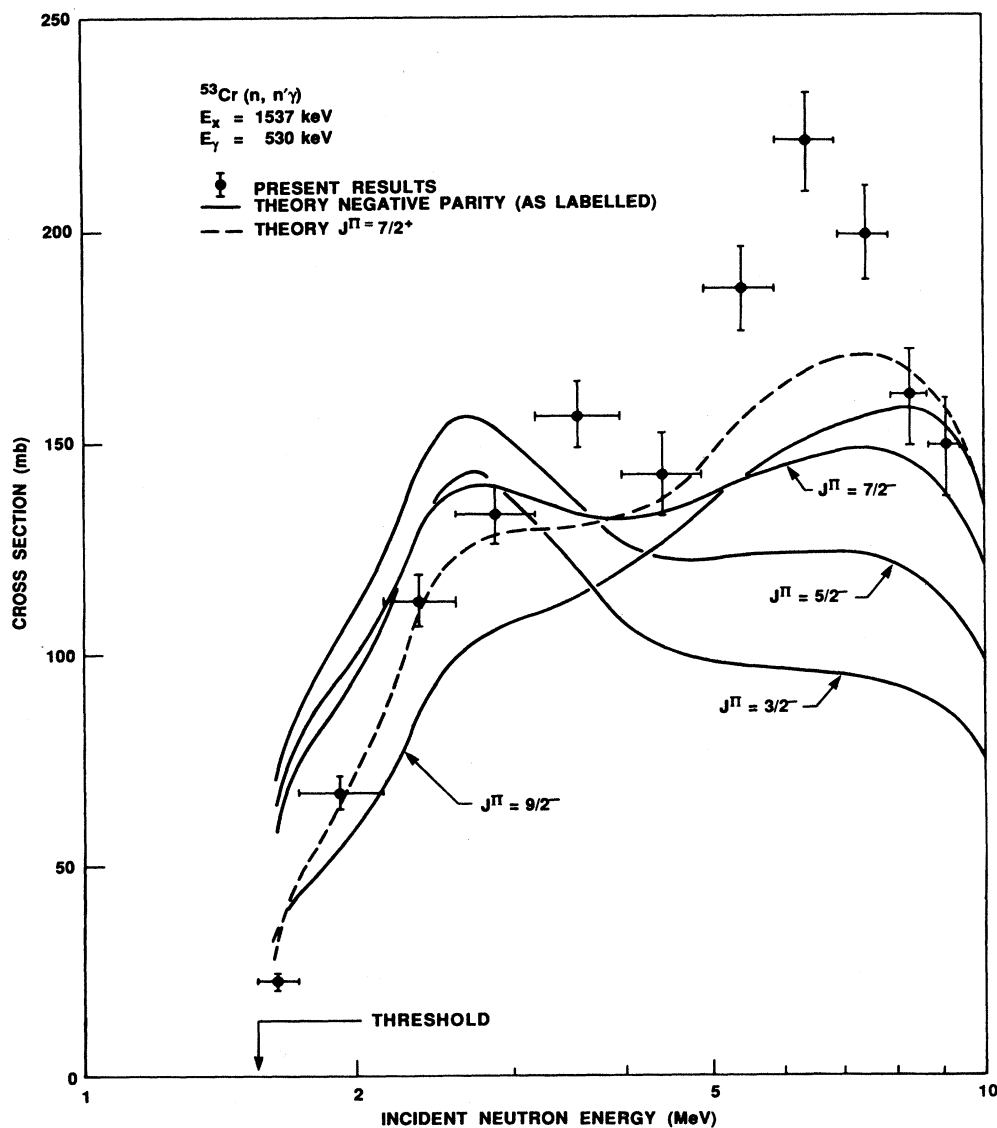

FIG. 18. Comparison of present experimental excitation function for $E_\gamma = 530$ keV following decay of the 1537-keV level in ^{53}Cr with statistical-model calculations for several choices for J^π assigned to this level. The calculated curve giving the best representation of the data is for an assignment of $J^\pi = \frac{7}{2}^+$, but, as discussed in the text, a positive-parity level is not known experimentally, nor expected theoretically on the basis of shell-model systematics, at this low an excitation energy in ^{53}Cr.

do not suggest that a positive-parity level in fact exists at this low excitation energy in ^{53}Cr, but only that some care must be taken when interpreting excitation functions within the framework of the statistical model. The $E_x = 1537$-keV level is clearly a difficult level to understand; the discrepancies in Figs. 9 and 10 are not the only inconsistencies that need to be resolved.

V. CONCLUSIONS AND RECOMMENDATIONS

One goal discussed in the Introduction has been met, and that is the goal to provide experimental cross sections for comparisons with predictions of nuclear-model calculations. Comparisons with a recent theoretical study,[55] as shown in Figs. 5–7, 11, and 15, are very adequate for $E_n < 4$ MeV, and quite encouraging for $E_n > 4$ MeV. Only for $E_x = 1537$ keV, as shown in Figs. 9 and 18, is the comparison less favorable.

A second goal, to provide new or definitive level-structure nuclear data, has been met to a moderate degree. The present data have helped to clarify the status of the $E_x = 2453$-keV level as well as to provide a definitive separation of the doublet at $E_x \sim 2706$ keV. Some new decay transitions for levels having $E_x > 3$ MeV were observed, and these have been reported[49] in detail, including determination of a previously unreported level at $E_x = 3172 \pm 3$ keV. However, as shown in Fig. 12 there were several adopted[34] levels for which we could not confidently locate peaks (in our data) so as to assign transition gamma rays even for some levels having $E_x < 3$ MeV.

It appears to us that the level structure of ^{53}Cr is not as well understood as might be expected based on the amount of experimental and theoretical effort so far reported. We note that in general for ^{53}Cr level excitation energies are only moderately well reproduced by calculation; the electromagnetic observables are not well predicted. Indeed, of the 21 nuclei for which Mooy and Glaudemans[44] calculated results, ^{53}Cr has the poorest agreement with electromagnetic observables. In our opinion, further experimental study of the excitation and decay of levels in ^{53}Cr, particularly for the 1537-keV level, is fully warranted. Further theoretical study of this level scheme will likely require new experimental information. Indeed, one may well determine that a different theoretical approach is needed for a good quantitative understanding of the ^{53}Cr level structure.

ACKNOWLEDGMENTS

[1] A. MacGregor and G. Brown, Nucl. Phys. **88**, 385 (1966).

[2] M. N. Rao, J. Rapaport, A. Sperduto, and D. L. Smith, Nucl. Phys. **A121**, 1 (1968).

[3] C. A. Whitten, Jr., Phys. Rev. **156**, 1228 (1967).

[4] R. Bock, H. H. Duhm, R. Jahr, R. Santo, and R. Stock, Phys. Lett. **19**, 417 (1965).

[5] J. H. Bjerregaard, P. F. Dahl, O. Hansen, and G. Sidenius, Nucl. Phys. **51**, 641 (1964).

[6] W. Fitz, J. Heger, R. Jahr, and R. Santo, Z. Phys. **202**, 109 (1967).

[7] J. R. Meriwether, I. Gabrielli, D. L. Hendrie, J. Mahoney, and B. G. Harvey, Phys. Rev. **146**, 804 (1966).

[8] Yu. A. Aleksandrov, A. E. Antropov, M. V. Aprelov, P. P. Zarubin, R. D. Ioannu, B. N. Orlov, and V. S. Romanov, Izv. Akad. Nauk SSSR, Ser. Fiz. **36**, 2648 (1972) [Bull. Acad. Sci. USSR, Phys. Ser. **36**, 2297 (1973)].

[9] P. David, H. H. Duhm, R. Bock, and R. Stock, Nucl. Phys. **A128**, 47 (1969).

[10] M. Borsaru, J. Nurzynski, D. W. Gebbie, C. L. Hollas, C. Whineray, N. H. Merrill, L. O. Barbopoulos, and A. R. Quinton, Nucl. Phys. **A237**, 93 (1975).

[11] J. Kawa, K. Okada, and T. Yamagata, J. Phys. Jpn. **36**, 929 (1974).

[12] R. N. Boyd, G. D. Gunn, H. Clement, W. P. Alford, T. Taylor, P. Ikossi, and J. A. Cameron, Nucl. Phys. **A277**, 119 (1977).

[13] R. L. Kozub, C. B. Chitwood, D. J. Fields, C. J. Lister, and E.

K. Warburton, Phys. Rev. C **30**, 1324 (1984).

[14] W. Eyrich, S. Schneider, A. Hofmann, U. Scheib, and F. Vogler, Phys. Rev. C **10**, 2512 (1974).

[15] D. M. Van Patter, N. Nath, S. M. Shafroth, S. S. Malik, and M. A. Rothman, Phys. Rev. **128**, 1246 (1962).

[16] G. A. Bartholomew and M. R. Gunye, Can. J. Phys. **43**, 1128 (1965).

[17] T. P. G. Carola, W. C. Olsen, D. M. Sheppard, B. D. Sowerby, and P. J. Twin, Nucl. Phys. **A144**, 53 (1970).

[18] D. L. Broder, A. F. Gamalii, B. V. Zemtsev, B. V. Nesterov, and L. P. Kham'yanov, Yad. Fiz. **13**, 233 (1971) [Sov. J. Nucl. Phys. **13**, 129 (1971)].

[19] T. P. Carola and J. G. Tamboer, Nucl. Phys. **A185**, 81 (1972).

[20] L. C. McIntyre, Jr. and D. J. Donahue, Phys. Rev. C **6**, 568 (1972).

[21] J. Kopecky, K. Abrahams, and F. Stecher-Rasmussen, Nucl. Phys. **A188**, 535 (1972).

[22] W. Gullholmer and Z. P. Sawa, Nucl. Phys. **A204**, 561 (1973).

[23] P. Engelstein, M. Forterre, N. Schulz, and J. P. Vivien, Nucl. Phys. **A230**, 358 (1974).

[24] A. R. Poletti, B. A. Brown, D. B. Fossan, and E. K. Warburton, Phys. Rev. C **10**, 2312 (1974).

[25] G. Tessler and S. S. Glickstein, *Proceedings of the Conference on Nuclear Cross Sections and Technology, Washington, D.C., 1975*, Natl. Bur. Stand. (U.S.) Spec. Publ. No. 425, edited by R. A. Schrack and C. D. Bowman (NBS Washington, D.C., 1975), p. 934.

[26]P. N. Patrawale and R. G. Kulkarni, J. Phys. G. **3**, 1245 (1977).

[27]P. T. Karatzas, G. P. Couchell, B. K. Barnes, L. E. Beghian, P. Harihar, A. Mittler, D. J. Pullen, E. Sheldon, and N. B. Sullivan, Nucl. Sci. Eng. **67**, 34 (1978).

[28]E. K. Warburton, J. W. Olness, A. M. Nathan, and A. R. Poletti, Phys. Rev. C **18**, 1637 (1978).

[29]D. C. Radford and A. R. Poletti, J. Phys. G **5**, 409 (1979).

[30]J. Kopecky, R. E. Chrien, and H. I. Liou, Nucl. Phys. **A334**, 35 (1980).

[31]A. P. Byrne and A. R. Poletti, Nucl. Instrum. Methods **193**, 489 (1982).

[32]L. Dorikens-Vanpraet, M. Dorikens, and J. Demuynck, Z. Phys. **241**, 459 (1971).

[33]T. E. Ward, P. H. Pile, and P. K. Kuroda, Nucl. Phys. **A134**, 60 (1969).

[34]L. K. Peker, Nucl. Data Sheets **43**, 481 (1984).

[35]J. Vervier, Nucl. Phys. **78**, 497 (1966).

[36]K. Ramavataram, Phys. Rev. **132**, 2255 (1963).

[37]J. R. Maxwell and W. C. Parkinson, Phys. Rev. **135**, B82 (1964).

[38]H. Ohnuma, Nucl. Phys. **88**, 273 (1966).

[39]R. J. Philpott and W. W. True, Phys. Rev. C **2**, 512 (1970).

[40]D. Larner, Phys. Rev. C **2**, 522 (1970).

[41]T. P. G. Carola and H. Ohnuma, Nucl. Phys. **A165**, 259 (1971).

[42]H. Horie and K. Ogawa, Prog. Theor. Phys. **46**, 439 (1971).

[43]H. G. Benson and I. P. Johnstone, Can. J. Phys. **54**, 1683 (1976); I. P. Johnstone and H. G. Benson, J. Phys. G **3**, L69 (1977).

[44]R. B. M. Mooy and P. W. M. Glaudemans, Z. Phys. A **312**, 59 (1983).

[45]J. B. McGrory (private communication); see J. B. McGrory, Phys. Lett. **21**, 64 (1966).

[46]Z. W. Bell, J. K. Dickens, D. C. Larson, and J. H. Todd, Nucl. Sci. Eng. **84**, 12 (1983); D. C. Larson, in *Nuclear Data for Basic and Applied Science*, Proceedings of the International Conference, edited by P. G. Young, R. E. Brown, G. F. Auchampaugh, P. W. Lisowski, and L. Stewart (Gordon and Breach, New York, 1986), p. 71.

[47]P. E. Hodgson, in *Proceedings of the International Conference on Nuclear Data for Science and Technology*, edited by S. Igarasi (Saikon, Tokyo, 1988), p. 655.

[48]D. M. Hetrick, C. Y. Fu, and D. C. Larson, in *Nuclear Data for Basic and Applied Science*, Proceedings of the International Conference, edited by P. G. Young, R. E. Brown, G. F. Auchampaugh, P. W. Lisowski and L. Stewart (Gordon and Breach, New York, 1986), p. 1197; P. G. Young, E. D. Arthur, and D. G. Madland, *Proceedings of the Conference on Nuclear Cross Sections and Technology, Knoxville, 1979*, Natl. Bur. Stand. (U.S.) Spec. Publ. No. 594, edited by J. L. Fowler, C. H. Johnson, and C. D. Bowman (U.S. GPO, Washington, D.C., 1980), p. 639.

[49]J. K. Dickens and D. C. Larson, Oak Ridge National Laboratory Report No. ORNL-6418, 1987.

[50]S. R. de Groot, H. A. Tolhoek, and W. J. Huiskamp, in *Alpha, Beta, and Gamma-Ray Spectroscopy*, edited by K. Siegbahn (North-Holland, Amsterdam, 1965), Vol. 2, p. 1199; E. Sheldon and D. M. Van Patter, Rev. Mod. Phys. **38**, 1943 (1966).

[51]J. K. Dickens, Nucl. Instrum. Methods **98**, 451 (1972).

[52]E. Storm and H. I. Israel, Nucl. Data Tables A7, 565 (1970).

[53]C. Y. Fu, Oak Ridge National Laboratory Report No. ORNL/TM-7402, 1980 (unpublished); C. Y. Fu, Nucl. Sci. Eng. **86**, 344 (1984); **92**, 440 (1986); K. Shibata and C. Y. Fu, Oak Ridge National Laboratory Report No. ORNL/TM-10093, 1986 (unpublished).

[54]P. D. Kunz, distorted wave code DWUCK−72, University of Colorado (unpublished).

[55]K. Shibata and D. M. Hetrick, Oak Ridge National Laboratory Report No. ORNL/TM-10381, 1987 (unpublished).

[56]B. H. Wildenthal, *Proceedings of the International School of Nuclear Physics, Erice, Italy*, Vol. 11 of *Progress in Particle and Nuclear Physics*, edited by D. Wilkinson (Pergamon, Oxford, 1982).

[57]R. L. Auble, Nucl. Data Sheets **21**, 323 (1977).

[58]W. Hauser and H. Feshbach, Phys. Rev. **87**, 366 (1952).

[59]E. H. Auerbach and F. G. J. Perey, Brookhaven National Laboratory Report No. BNL-765, 1962 (unpublished).